Inorganic Chemistry

Article

pubs.acs.org/IC

A Versatile Dinucleating Ligand Containing Sulfonamide Groups

Jonas Sundberg,[†] Hannes Witt,[†] Lisa Cameron,[†,‡] Mikael Håkansson,[§] Jesper Bendix,[⊥] and Christine J. McKenzie*[,†]

[†]Department of Physics, Chemistry and Pharmacy, University of Southern Denmark, Campusvej 55, 5230 Odense M, Denmark

[‡]School of Chemistry, The University of Sydney, NSW 2006, Australia

[§]Department of Chemistry and Molecular Biology, University of Gothenburg, SE-412 96 Gothenburg, Sweden

[⊥]Department of Chemistry, University of Copenhagen, Universitetsparken 5, 2100 Copenhagen, Denmark

Supporting Information

ABSTRACT: Copper, iron, and gallium coordination chemistries of the new pentadentate bis-sulfonamide ligand 2,6-bis(*N*-2-pyridylmethylsulfonamido)-4-methylphenol ($psmpH_3$) were investigated. $PsmpH_3$ is capable of varying degrees of deprotonation, and notably, complexes containing the fully trideprotonated ligand can be prepared in aqueous solutions using only divalent metal ions. Two of the copper(II) complexes, $[Cu_2(psmp)(OH)]$ and $[Cu_2(psmp)(OAc)_2]^-$, demonstrate the anticipated 1:2 ligand/metal stoichiometry and show that the dimetallic binding site created for exogenous ligands possesses high inherent flexibility since additional one- and three-atom bridging ligands bridge the two copper(II) ions in each complex, respectively. This gives rise to a difference of 0.4 Å in the Cu···Cu distances. Complexes with 2:3 and 2:1 ligand/metal stoichiometries for the divalent and trivalent metal ions, respectively, were observed in $[Cu_3(psmp)_2(H_2O)]$ and $[M(psmpH)(psmpH_2)]$, where M = Ga^{III}, Fe^{III}. The deprotonated tridentate *N*-2-pyridylsulfonylmethylphenolato moieties chelate the metal ions in a meridional fashion, whereas in $[Cu_3(psmp)_2(H_2O)]$ the rare μ_2-*N*-sulfonamido bridging coordination mode is observed. In the bis-ligand mononuclear complexes, one picolyl arm of each ligand is protonated and uncoordinated. Magnetic susceptibility measurements on the doubly and triply bridged dicopper(II) complexes indicate strong and medium strength antiferromagnetic coupling interactions, with J = 234 cm^{-1} and 115 cm^{-1} for $[Cu_2(psmp)(OH)]$ and $[Cu_2(psmp)(OAc)_2]^-$, respectively (in H_{HDvV} =...+JS_1S_2 convention). The trinuclear $[Cu_3(psmp)_2(H_2O)]$, in which the central copper ion is linked to two flanking copper atoms by two μ_2-*N*-sulfonamido bridges and two phenoxide bridges shows an overall magnetic behavior of antiferromagnetic coupling. This is corroborated computationally by broken-symmetry density functional theory, which for isotropic modeling of the coupling predicts an antiferromagnetic coupling strength of J = 70.5 cm^{-1}.

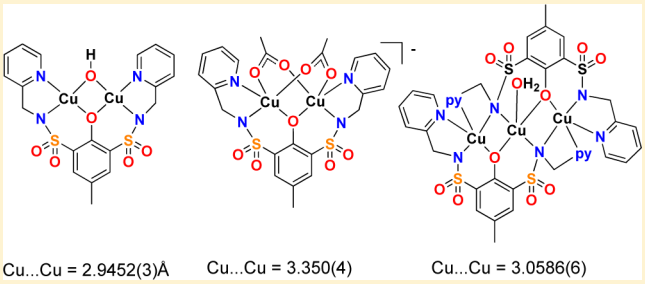

INTRODUCTION

Acyclic dinucleating ligands are of continued interest for the preparation of complexes that bind exogenous molecules at preorganized "dimetallic sites." Coordination at these sites has, in some cases, resulted in the labile exogenous guests showing enhanced reactivity, and some proposed mechanisms of reactions are reminiscent of those for the dinuclear metalloenzymes.[1] Clearly features of the supporting ligand, like donor atoms and charge, denticity, chelate ring size, bite angles, and other steric factors will influence the metal ion geometries and M···M distances and consequently tune the coordination chemistry of a preorganized dimetallic active site. One of the largest classes of acyclic and macrocyclic dinucleating ligands are constructed around bis-ortho functionalized, potentially bridging phenolato groups. Readily accessible frameworks for acyclic systems of this type of ligand utilize a Schiff base condensation of 2,6-diformyl-4-methylphenol with amines containing other donor groups, for example 2-(aminomethyl)-pyridine (Scheme 1a).[2] We were interested in conserving this particular framework, but to modify it by including anionic donors trans to the sites in which the exogenous ligands will bind in derived dimetallic complexes. The intention was to subsequently exploit the resultant lower overall positive charge of the complex and trans effect in influencing the reactivity of coordinated guests. This construction might be expected to give scope for accessing dinuclear complexes with high-valent metal ions. A desirable outcome is opening up new metal cooperativity vistas in the field of the catalysis of oxidation reactions by first-row transition metals.

Scheme 1

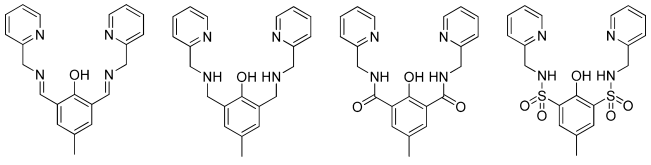

Received: October 15, 2013
Published: February 28, 2014

 © 2014 American Chemical Society dx.doi.org/10.1021/ic402599e | *Inorg. Chem.* 2014, 53, 2873−2882

By analogy dianionic macrocycles and chelates like porphyrins and salens have been benchmarks in the history of the development of monometallic catalysts for oxidation reactions. At the other end of the spectrum, the coordination of low-valent metal ions by such ligands might have potential for the activation of electrophilic guests bound at the dimetallic site. To this end we speculated that the fully deprotonated forms of the ligands in Scheme 1b–d were candidates for the construction of dinuclear complexes containing the same donor set, but with 3 times the negative charge of the deprotonated ligand in Scheme 1a.

It is reasonable to assume that the deprotonation of the known bis-secondary amine ligand[3] (Scheme 1b) is unlikely to occur in the presence of water, and the use of nonaqueous solvents, anhydrous metal sources, and prior deprotonation by very strong bases (e.g., alkyllithium reagents) are required for the preparation of metal complexes. Even if complexes were isolated these are likely to be easily hydrolyzed, and protonation of the amido groups would occur. Thus we considered that the approach of introducing secondary amide groups is more practical. It is well-established that deprotonation and N coordination of secondary carboxamido groups in chelating and macrocyclic ligands to metal ions is facile even in water, despite unfavorable pK_a values. The strong amido–N–σ donor capability is important for the tetraamido macrocycles, developed by Collins and co-workers, which have proved to be important ligands for the purpose of stabilizing mononuclear high-valent iron complexes.[4,5] Using this class of ligand, Fe(IV)oxo[4] and the first Fe(V)oxo[5] species have been identified, and these complexes have been exploited for the catalysis of the oxidation of organic substrates. The early studies by Stephens and Vagg and co-workers demonstrated that tetradentate diamide ligands could be deprotonated and employed successfully under aqueous conditions for the formation of mononuclear intermediate valent complexes.[6] The dicarboxamide pro-ligand in Scheme 1c was, however, not deprotonated in a zinc complex.[7] Given this outcome, and the fact that the pK_a values of neutral primary and secondary sulfonamides (pK_a approximately 7–16) can be several orders of magnitude lower than for the analogous carboxamides (pK_a approximately 12–27), we turned our sights to the synthesis of the previously unknown bis-sulfonamide pro-ligand, Scheme 1d. Apart from the more favorable acid–base chemistry, sulfonamide groups have not been extensively employed as central –R–SO_2–N– components in chelating ligands. They must, however, be attractive in terms of their charge versatility; sulfonamide donors can be dianionic,[8,9] monoanionic,[10] or neutral.[11] The majority of the known sulfonamide-containing ligands are derived from tosylation of the parent amine-functionalized ligands; consequently, the –R–SO_2–N– moiety terminates and does not form part of a chelate. Therefore, known complexes do not provide predictive models for the way in which the potentially dinucleating bis-sulfonamide pro-ligand, 2,6-bis(*N*-2-pyridylmethylsulfonamido)-4-methylphenol ($psmpH_3$), in Scheme 1d might be expected to coordinate in metal complexes. We report here the synthesis of $psmpH_3$ and the characterization of a remarkable range of topologies in its coordination complexes.

RESULTS AND DISCUSSION

The pro-ligand 2,6-bis(*N*-2-pyridylmethylsulfonamide)-4-methylphenol ($psmpH_3$) is prepared by a 2:1 condensation of 2-aminopyridine and 2,6-dichlorosulfone-4-methylphenol (Scheme 2) and is isolated in good yields as an air- and moisture-stable off-white powder.

Scheme 2

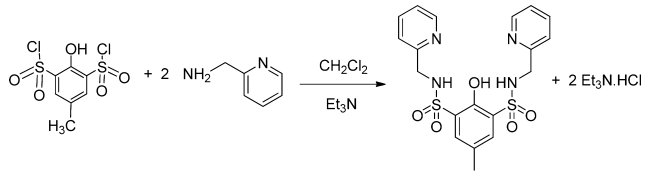

Reactions of $psmpH_3$ with 2 equiv of copper(II) acetate in CH_2Cl_2, CH_3CN, MeOH, EtOH, or water all resulted in the immediate formation of relatively insoluble solids with various greenish-blue hues. Bands between 1000 and 1400 cm^{-1} in their IR spectra can be associated with the sulfonamide groups. Small variations could be correlated to differences in color. Inspection of the crystalline solids using a light microscope showed that solids were in general mixtures containing two or three different crystal types. The least soluble of these solids, oblong dark blue crystals, were the most thermodynamically stable crystalline product. Mixtures of crystals that redissolved in mother liquor or were dissolved in fresh solvent were prone to convert to this form if allowed to stand for a prolonged period of time under ambient conditions. This process is accelerated by addition of small amounts of NaOH (1 equiv per ligand) or by diffusion of ammonia into the solutions. An olive-green solid obtained from the reactions performed in dichloromethane was the only material that showed vibrations that could be attributed to the incorporation of an acetato ligand, despite the presence of acetate in all reactions. At 1601 and 1410 cm^{-1}, for asymmetric and symmetric carboxylato stretching, respectively, the difference of 191 cm^{-1} was consistent with a μ_2-acetato group.[12] Corroborating this, the negative-ion electrospray ionization mass spectrometry (ESI-MS) shows a base peak at m/z 690.96, which can be assigned to $[Cu_2(psmp)(OAc)_2]^-$, suggesting the presence of this ion in the material. The issue of a charge-balanced formulation was first resolved by single-crystal X-ray diffraction, vide infra, showing that the unexpected countercation, $[N(Et)_3CH_2Cl]^+$, had been formed from the reaction between triethylamine and CH_2Cl_2.[13] Despite this, the preparation of $[N(Et)_3CH_2Cl][Cu_2(psmp)(OAc)_2]$ is entirely repeatable. Attempts to prepare $[Cu_2(psmp)(OAc)_2]^-$ in salts with alternative, deliberately added, and similarly sized counterions, for example, Et_4N^+, by reactions where triethylamine and/or CH_2Cl_2 were omitted, produce powders that, according to spectroscopy, contained the same complex anion.

As mentioned above acetato bands were absent in the IR spectra of dark-blue and grass-green crystals obtained from the aforementioned reactions. What appeared to be very similar materials by comparisons of their IR spectra could also be obtained using copper(II) nitrate and copper(II) sulfate as the starting materials. Thus it could be concluded that none of the acetate, nitrate, or sulfate were components of these two different products, and that they were most likely neutral compounds. Positive-ion ESI mass spectra were obtained only for the slightly more soluble grass-green materials; however, the spectra were not particularly informative inasmuch as they contained several ions assignable to species containing 1:1, 1:2, and 3:2 ligand/copper stoichiometries. Optimization of reaction conditions finally produced pure batches of well-defined crystalline materials of the dark-blue and grass-green copper complexes.

The structures of the three different copper(II) compounds, which in practice can cocrystallize from the 2:1 reaction of copper acetate and $psmpH_3$, were determined by single-crystal

dx.doi.org/10.1021/ic402599e | Inorg. Chem. 2014, 53, 2873–2882

X-ray diffraction to be $[Cu_2(psmp)(OH)]$ (blue oblong crystals), $[N(Et)_3CH_2Cl][Cu_2(psmp)(OAc)_2]\cdot 2CH_2Cl_2$ (olive-green crystals), and $[Cu_3(psmp)_2(H_2O)]\cdot H_2O$ (grass-green crystals). Their molecular structures are shown in Figure 1a–c.

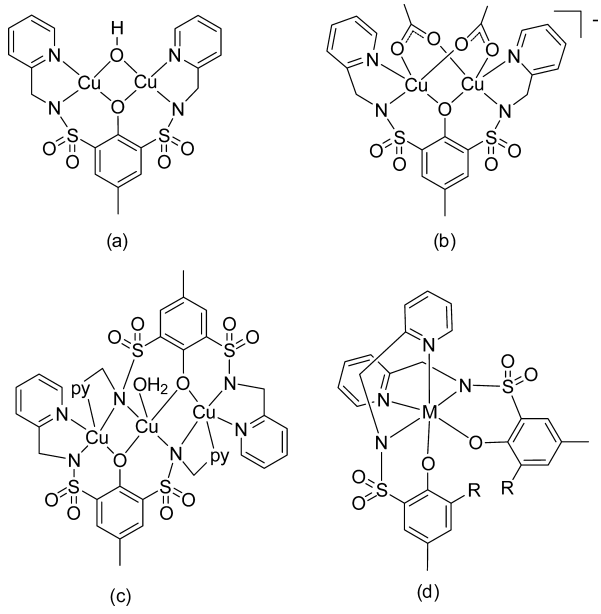

Figure 1. Chemical diagrams of the complexes of fully or partially deprotonated 2,6-bis(*N*-2-pyridylmethyl-sulfonamide)-4-methylphenol ($psmpH_3$) found in (a) $[Cu_2(psmp)(OH)]$, (b) $[N(Et)_3CH_2Cl][Cu_2(psmp)(OAc)_2]\cdot 2CH_2Cl_2$, (c) $[Cu_3(psmp)_2(H_2O)]\cdot H_2O$, and (d) $[M(psmpH)(psmpH_2)]$. R = $-SO_2NCH_2py$, M = Fe^{III} or Ga^{III}.

These contrasting structures conclusively demonstrate that all of the potential sulfonamide donors of $psmpH_3$ are deprotonated and that the N atom is coordinated to the copper(II) ions. As mentioned above the addition of hydroxide or ammonia to any of the reaction mixtures leads ultimately to the formation of the blue compound, which we could now assign to the very insoluble $[Cu_2(psmp)(OH)]$. Thus it can be surmised that deprotonation of the water ligand of the neutral 2:3 ligand/metal complex $[Cu_3(psmp)_2(H_2O)]$ does not produce its deprotonated congener $[Cu_3(psmp)_2(OH)]^-$; rather, a rearrangement occurs, and the neutral 1:2 ligand/metal species $[Cu_2(psmp)(OH)]$ is formed, consistent with the fact that hydroxide ligands prefer bridging over terminal coordination.

The outcome of the reactions of gallium(III) and iron(III) salts with $psmpH_3$ contrasts to the reactions with the divalent metal ions. Even in the presence of more than two metal ions per $psmpH_3$ the neutral bis-ligand mononuclear complexes $[M(psmpH)(psmpH_2)]$ are isolated (Figure 1d). In these, one tridentate $N_{py}N_{sulfonamide}O_{phenol}$ half of each ligand binds the octahedral ion meridionally, while the other half of each ligand is uncoordinated and protonated. This result was unanticipated given that the more highly electropositive metals ions, compared to Cu^{2+}, might be expected to outcompete protons.

The crystal structure of $[Cu_3(psmp)_2(H_2O)]$ shows an elongation of the S–N bond of the bridging sulfonamides compared to the sulfonamide involved in meridional chelation of one metal ion. The former bond distance is comparable to the one found in the structure of the free ligand, as well as the uncoordinated sulfonamides in $[M(psmpH)(psmpH_2)]$ (M = Ga^{III} or Fe^{III}). Otherwise the crystal structures show that the S–O distances are essentially unaffected by coordination of sulfonamide. Accordingly many of the bands in the relevant region of the IR spectra are similar throughout the series, and this technique was not particularly diagnostic of the structure of these relatively insoluble compounds.

X-RAY CRYSTAL STRUCTURES

The molecular structures of $psmpH_3$, $[Cu_2(psmp)(OH)]$, $[Cu_2(psmp)(OAc)_2]^-$, $[Cu_3(psmp)_2(H_2O)]$, $[Ga(psmpH)(psmpH_2)]$, and $[Fe(psmpH)(psmpH_2)]$ were determined by single-crystal X-ray diffraction and are shown in Figures 2–6. A

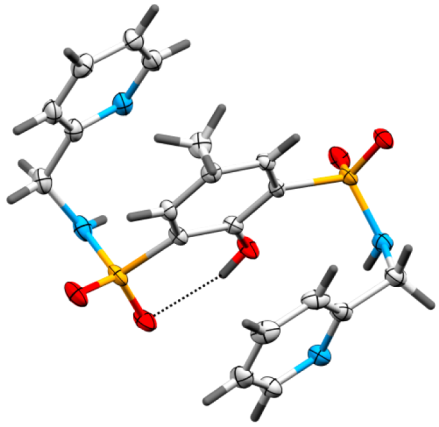

Figure 2. Molecular structure of $psmpH_3$. Anisotropic displacement parameters are drawn at the 50% probability level.

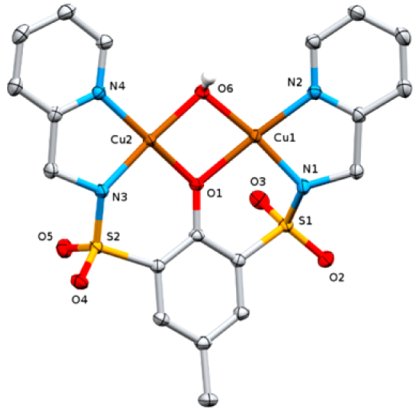

Figure 3. Molecular structure of $[Cu_2(psmp)(OH)]$. Anisotropic displacement parameters are drawn at the 50% probability level. Apart from that bound to O6, the hydrogen atoms are omitted for clarity.

summary of bond distances and angles for the complexes can be found in Tables 1–3. The structure of the free ligand, $psmpH_3$, shows a conformation in which the pyridyl arms are twisted approximately 180° relative to each other above and below the plane of the phenol ring to give a slightly offset intramolecular π-stacking (Figure 2). The phenol hydroxyl H atom H-bonds to a sulfonyl O (2.770 Å). The structures of neutral $[Cu_2(psmp)(OH)]$ (Figure 3) and anionic $[Cu_2(psmp)(OAc)_2]^-$ (Figure 4) demonstrate conclusively that this new bis-sulfonamide ligand forms the intended dinuclear complexes. The conformation of the ligand has changed dramatically compared to its protonated precursor. Furthermore the $[M_2(psmp)]^+$ scaffold is flexible enough to accommodate the extremes of auxiliary one-atom and three-atom bridging groups. The incorporation of a hydroxido or two acetato

dx.doi.org/10.1021/ic402599e | *Inorg. Chem.* 2014, 53, 2873–2882

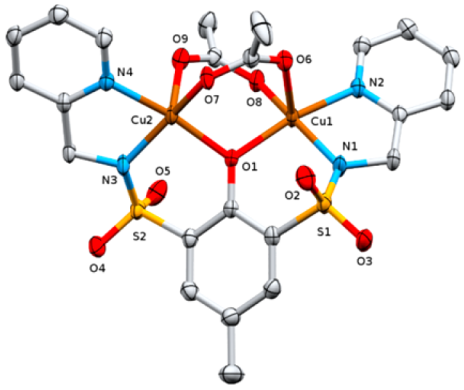

Figure 4. Molecular structure of the of the anion in $[N(Et)_3CH_2Cl]$-$[Cu_2(psmp)(OAc)_2]$. Anisotropic displacement parameters are drawn at the 50% probability level. Hydrogen atoms omitted for clarity.

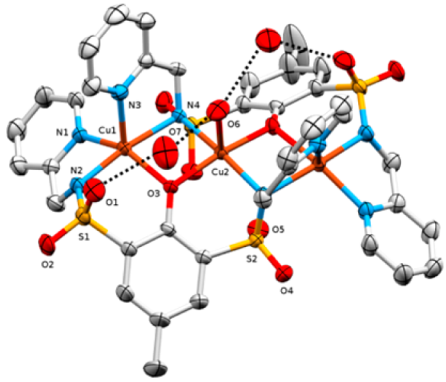

Figure 5. Molecular structure of $[Cu_3(psmp)_2(H_2O)]$. Anisotropic displacement parameters are drawn at the 50% probability level. The noncoordinated water molecule site occupation is 50%. Hydrogen atoms omitted for clarity.

bridges is associated with square planar and distorted square pyramidal geometries and intermetallic distances of 2.9452(3) and 3.350(4) Å, respectively. The former distance is similar to that found in dicopper(II) complexes of the Schiff base ligand in Scheme 1a, while the latter is significantly larger and consistent with the presence of two three-atom bridges—a construction that in fact has not yet been identified for the Schiff base ligand in Scheme 1a. The deprotonated sulfonamide groups central in the tridentate meridional arrangement of each arm coordinate via the N atoms. The dihedral angle between the basal CuN_2O_2 planes of the distorted square pyramidal copper ions in $[Cu_2(psmp)$-$(OAc)_2]$ is approximately 95°.

In the structure of $[Cu_3(psmp)_2(H_2O)]$, the two $psmp^{3-}$ ligands bind to all three linearly oriented copper ions by forming a double helix around them (Figure 5). A deprotonated sulfonamide N atom from each half of each ligand forms μ_2 bridges between the central copper and one flanking copper ion. The other half of each ligand meridionally chelate each flanking copper(II) ion. The basal planes of the three copper ions are coplanar and linearly orientated, with the apical positions filled by the pyridine N for the two terminal copper ions and an exogenous water ligand for the central copper ion. The Cu···Cu distances are 3.0586(6)Å. The coordinated water group is contained within a well-defined cleft surrounded by two pyridyl rings and two sulfonamide groups, a second water molecule situated between the coordinated H_2O and surrounding sulfonamide oxygen atom stabilizes the conformation via hydrogen bonding.

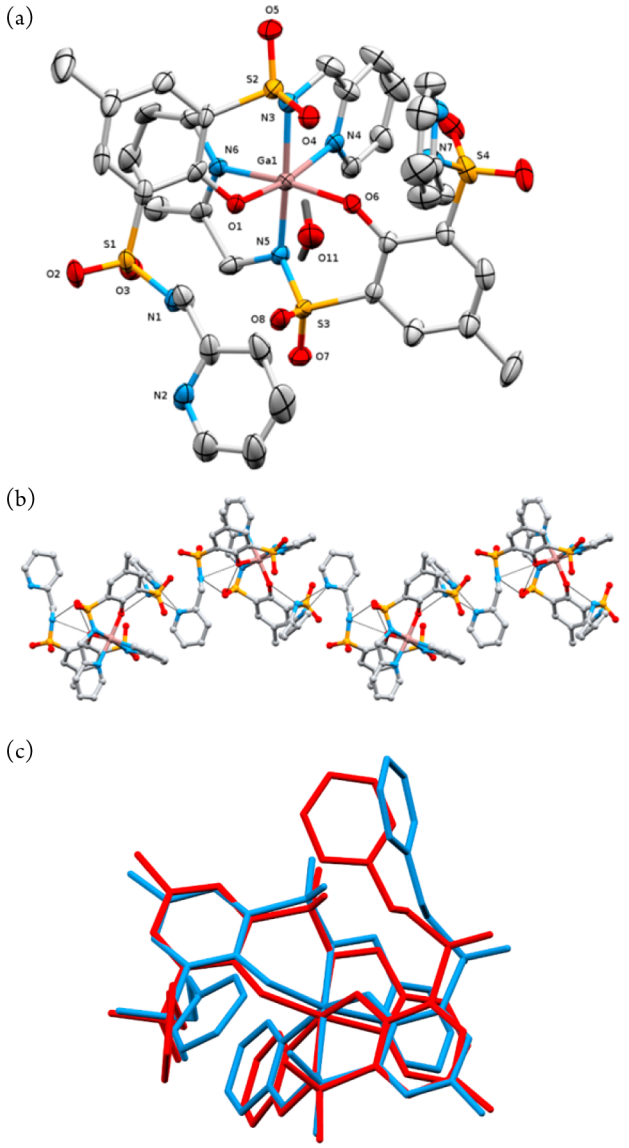

Figure 6. (a) Molecular structure of $[Ga(psmpH)(psmpH_2)]$. Anisotropic displacement parameters are drawn at the 50% probability level. Hydrogen atoms omitted for clarity. (b) Packing diagram of $[Ga(psmpH)(psmpH_2)]$ showing H-bonded chains along the *a* axis. (c) Molecular overlay of (red) $[Fe(psmpH)(psmpH_2)]$ and (blue) $[Ga(psmpH)(psmpH_2)]$.

The structure of $[Ga(psmpH)(psmpH_2)]$ (Figure 6a) shows the Ga(III) ion is octahedrally coordinated by two tridentate meridional $pyCH_2NS(O)_2$phenolato groups of the two ligands. The deprotonated sulfonamide N atoms of each ligand are orientated trans to each other. The phenolato O of one ligand and pyridine N donors of the second are trans to each other. The uncoordinated sulfonamide and pyridine N donors are protonated and are involved in a H-bonded chain of molecules along the *a* axis (Figure 6b). The lattice water is encased in a cavity surrounded by a sulfonamide O atom (H_2O···O4 = 2.956(7)Å), the phenolato O atom (H_2O···O1 = 3.055(7)Å), and a pyridine CH group (H_2O···C = 3.270(1)Å), all belonging to a single psmp unit. The iron complex is structurally identical, with an analogous hydrogen-bonding pattern. An overlay of the crystal structures of the Ga(III) and Fe(III) complexes is shown in Figure 6c.

dx.doi.org/10.1021/ic402599e | *Inorg. Chem.* 2014, 53, 2873−2882

Table 1. Selected Bond Distances (Å) and Angles (deg) for $[Cu_2(psmp)(OH)]$ and $[Cu_2(psmp)(OAc)_2]^-$

	$[Cu_2(psmp)(OH)]$	$[Cu_2(psmp)(OAc)_2]^-$
Cu1−O1	2.0102(10)	2.003(3)
Cu2−O1	1.9499(11)	2.018(3)
Cu1···Cu2	2.9452(3)	3.350(4)
Cu1−N1	1.8989(13)	1.944(3)
Cu1−N2	1.9709(13)	2.034(3)
Cu2−N3	1.9183(12)	1.943(4)
Cu2−N4	1.9632(12)	2.037(3)
S1−O2	1.4459(11)	1.443(4)
S1−O3	1.4523(12)	1.451(3)
S2−O4	1.4588(11)	1.455(3)
S2−O5	1.4498(12)	1.451(4)
S1−N1	1.585(4)	1.570(4)
S2−N3	1.596(4)	1.576(4)
O1−Cu1−O6	79.87(4)	97.48(12)
O1−Cu1−N1	94.06(5)	93.59(13)
O1−Cu1−N2	172.46(5)	170.81(13)
N1−Cu1−N2	84.21(5)	80.92(14)
O1−Cu2−O6	80.89(4)	97.48(12)
O1−Cu2−N3	97.62(5)	93.05(13)
O1−Cu2−N4	171.07(5)	169.30(13)
N3−Cu2−N4	84.23(5)	80.94(14)
Cu1−O1− Cu2	96.08(4)	112.86(13)

Table 2. Selected Bond Distances (Å) and Angles (deg) for $[Cu_3(psmp)_2(H_2O)]$

	$[Cu_3(psmp)_2(H_2O)]$
Cu1−N1	2.085(3)
Cu1−N2	1.937(3)
Cu1−N3	2.122(3)
Cu1−N4	2.066(3)
Cu1−O3	2.091(3)
Cu1···Cu2	3.0586(6)
Cu2−O3	1.953(3)
Cu2−N4	2.059(3)
Cu2−O6	2.239(4)
Cu1···Cu2	3.0586(6)
S1···N2	1.572(3)
S2···N4	1.630(3)
Cu1−N4−Cu2	95.73(9)
Cu1−O3−Cu2	98.24(9)
N4−Cu2−O3	94.57(9)
N1−Cu1−N4	104.03(9)
N1−Cu1−N2	79.10(9)
N2−Cu1−O3	92.98(9)
N4−Cu1−03	80.98(9)
N4−Cu2−O4	84.54(9)

MAGNETIC SUSCEPTIBILITY

Variable-temperature magnetic susceptibility measurements for the three copper compounds were measured over the range of 2.0−300 K. The plots of $\chi_m T$ versus T show that the systems display medium to strong antiferromagnetic interactions (Figures 7 and 8). The plot for $[Cu_2(psmp)(OH)]$ shows $\chi_m T \approx 0.52$ cm^3 mol^{-1} K at room temperature (RT), which is significantly lower than 0.75 cm^3 mol^{-1} K, the high-temperature value expected for two uncoupled copper(II) ions. The fit employing the spin-Hamiltonian of eq 1

$$\hat{H} = \mu_B B\cdot[g_x(\hat{S}_{1,x} + \hat{S}_{2,x}) + g_y(\hat{S}_{1,y} + \hat{S}_{2,y}) + g_z(\hat{S}_{1,z} + \hat{S}_{2,z})] + J\hat{S}_1\cdot\hat{S}_2 \quad (1)$$

gives the relatively strong antiferromagnetic coupling of J = 234 cm^{-1}. Not unexpectedly, because of the square pyramidal geometries, acetate bridges, and larger Cu−Cu separation, the $[N(Et)_3CH_2Cl][Cu_2(psmp)(OAc)_2]\cdot 2CH_2Cl_2$ compound shows weaker antiferromagnetic coupling, with J = 115 cm^{-1} and a $\chi_m T$ value approaching at RT that for two uncoupled copper(II) ions.

Only a handful of complexes containing *N*-sulfonamide-bridged metal ions are known, and most are diamagnetic.[14] For this reason the extent to which this unusual bridging group can mediate superexchange pathways for magnetic interactions has not been explored. We found only one system that is comparable to ours, namely, a doubly μ_2-$N_{sulfonamide}$ bridged dicopper(II) complex.[15] This complex displayed a ferromagnetic interaction (J = −54 cm^{-1}) between the square planar d^9 centers and weak intermolecular antiferromagnetic interactions (J = 0.66 cm^{-1}). It was thus of some interest to investigate the magnetic properties of $[Cu_3(psmp)_2(H_2O)]\cdot H_2O$. Overall antiferromagnetism is evident in the $\chi_m T$ product of this complex, and the temperature dependence of the susceptibility varies between 0.47 and 1.15 cm^3 mol^{-1} K as expected for one and just below three unpaired electrons (with $g_{iso} \approx 2.2$, cf. also Supporting Information) at low and high temperature, respectively. Dominant antiferromagnetic coupling is in agreement with density functional theory (DFT) calculations, vide infra.

THEORETICAL MODELING

The neutral compound $[Cu_3(psmp)_2(H_2O)]$ was modeled computationally with a Zn substituted for one of the terminal copper ions. The hydrogen atoms on the central water ligand were placed in calculated positions. A broken-symmetry (BS) DFT (S = 0,1) calculation was performed to determine the magnetic coupling. The computed value for the isotropic exchange coupling parameter was J = 70.48 cm^{-1} ($+JS_1S_2$ convention). Interestingly, the shapes and magnitudes of the Mulliken spin densities were determined to be quite similar for the bridging oxygen from the phenolate (+0.026) and the nitrogen from the sulfonamide (+0.023) (Figure 9).

ELECTROCHEMISTRY

A cyclic voltammogram of $[Cu_3(psmp)_2(H_2O)]$, Figure 10, suggests irreversible redox chemistry. It is likely also complicated by the rearranged species that can exist, as shown through ESI-MS and isolation (e.g., "recrystallization" of $[Cu_3(psmp)_2(H_2O)]$ gives $[Cu^{II}_2(psmp)(OH)]$). However, a dominating process is assigned to an irreversible Cu(II) to Cu(III) oxidation at 1.276 V. We assume this to be associated with the central copper ion and that this is broadened because the auxiliary water ligand found in the solid state is labile, and the closely related species $[Cu_3(psmp)_2(H_2O)]$, $[Cu_3(psmp)_2(CH_3CN)]$, and $[Cu_3(psmp)_2]$ may well be present and all oxidized to a Cu(II)Cu(III)Cu(II) complex at about the same potential. Lability and Cu(III)−OH_2 acidity would be consistent also with the presence of irreversible reductions at −0.717, −0.368, −0.089 V versus Fc^+/Fc. When a reductive scan starting at 0 V was run, the irreversible reductions were not observed (see Supporting Information, Figure S22). In the case of processes involving the crystallographically characterized ion $[Cu_3(psmp)_2(H_2O)]$ a spontaneous deprotonatation of the

dx.doi.org/10.1021/ic402599e | Inorg. Chem. 2014, 53, 2873−2882

Table 3. Selected Bond Distances (Å) and Angles (deg) for [Ga(psmpH)(psmpH$_2$)] and [Fe(psmpH)(psmpH$_2$)]

	[Ga(psmpH)(psmpH$_2$)]·H$_2$O	[Fe(psmpH)(psmpH$_2$)]·3H$_2$O
M−O1	1.964(4)	1.9559(19)
M−O6	1.951(4)	1.9419(19)
M−N3	2.020(5)	2.059(2)
M−N4	2.123(5)	2.166(2)
M−N5	2.002(5)	2.064(2)
M−N6	2.105(5)	2.157(3)
S1−O2	1.433(4)	1.435(2)
S1−O3	1.441(5)	1.436(2)
S2−O4	1.458(4)	1.450(2)
S2−O5	1.454(4)	1.449(2)
S1−N1	1.618(5)	1.617(3)
S2−N3	1.582(5)	1.589(2)
O1−M−N3	92.07(19)	89.34(8)
O1−M−N4	169.97(18)	164.25(9)
O1−M−N5	92.77(19)	95.17(8)
O1−M−N6	90.84(17)	91.89(9)
O1−M−O6	93.90(16)	96.78(8)
O6−M−N3	94.34(18)	97.89(9)
O6−M−N4	90.46(17)	91.16(9)
O6−M−N5	91.76(17)	88.49(9)
O6−M−N6	170.25(17)	163.57(9)

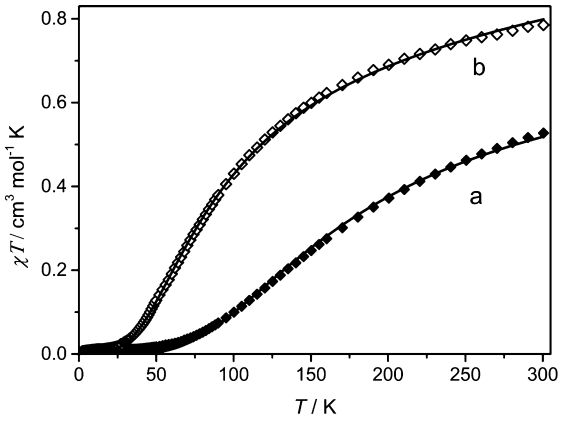

Figure 7. Variable-temperature magnetic susceptibility for (a) [Cu$_2$(psmp)(OH)] and (b) [N(Et)$_3$CH$_2$Cl][Cu$_2$(psmp)(OAc)$_2$]. The diamonds (◇) represent the experimental results, and the solid lines represent the best fits. Parameter values: (a) g_z = 2.14, g_x = g_y = 2.00 (fixed), J = 234 cm^{-1}; (b) g_z = 2.19, g_x = g_y = 2.00 (fixed), J = 115 cm^{-1}.

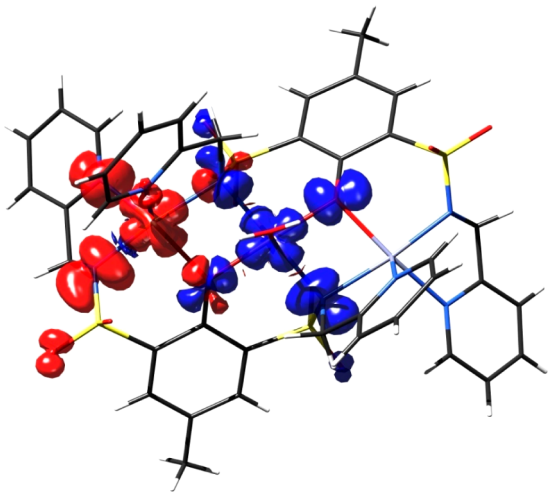

Figure 9. Computed spin densities for the BS state of the dinuclear model [Cu$_2$Zn(psmp)$_2$(H$_2$O)] with modeled water ligand. Plot is shown with isosurface values of ±1.3 × 10^{-3} Å^{-3}.

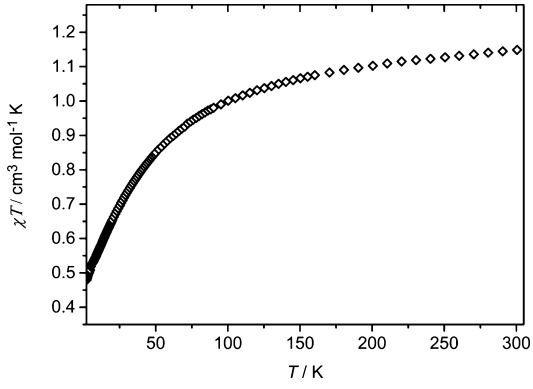

Figure 8. Variable-temperature magnetic susceptibility for [Cu$_3$(psmp)$_2$(H$_2$O)]·H$_2$O.

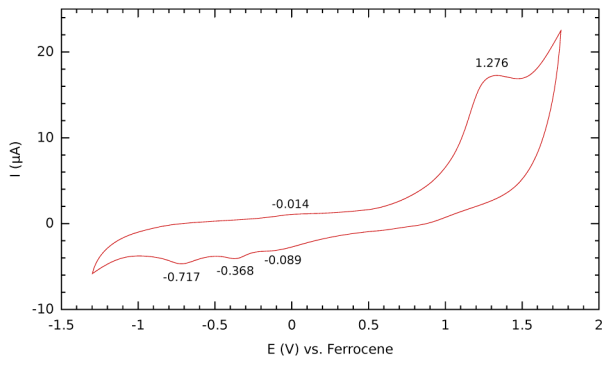

Figure 10. Cyclic voltammogram of [Cu$_3$(psmp)$_2$(H$_2$O)] in acetonitrile. Scan rate 100 mV s^{-1}, reference Fc$^+$/Fc.

dx.doi.org/10.1021/ic402599e | Inorg. Chem. 2014, 53, 2873−2882

water ligand after oxidation would give rise to irreversibility. The relevant reactions would be:

$$[Cu^{II}_3(psmp)_2(H_2O)] \rightarrow [Cu^{II}_2Cu^{III}(psmp)_2(H_2O)]^+ + e^-$$

$$[Cu^{II}_2Cu^{III}(psmp)_2(H_2O)]^+ \rightarrow [Cu^{II}_2Cu^{III}(psmp)_2(OH)] + H^+$$

Thus on re-reduction protonation of hydroxide ligand would subsequently occur:

$$[Cu^{II}_2Cu^{III}(psmp)_2(OH)] + e^- \rightarrow [Cu^{II}_3(psmp)_2(OH)]^-$$

$$[Cu^{II}_3(psmp)_2(OH)]^- + H^+ \rightarrow [Cu^{II}_3(psmp)_2(OH_2)]$$

Several redox processes are observed in acetonitrile solutions prepared from $[N(Et)_3CH_2Cl][Cu_2(psmp)(OAc)_2]$ (see Supporting Information, Figure S23). Acetate lability, and rearrangements to $[Cu_3(psmp)_2(H_2O)]$ and $[Cu_2(psmp)(OH)]$, as evident in the ESI-MS are feasible, and assignment was not attempted. $[Cu_2(psmp)(OH)]$ was too insoluble, and no signals could be observed. $[Fe(III)(psmpH)(psmpH_2)]$ shows an irreversible oxidation at 1.790 V and a quasi-reversible reduction centered at −1.15 V (see Supporting Information, Figure S24). The first process is not present in the cyclic voltammogram (CV) of the isovalent Ga complex and is therefore assigned to a Fe(III)/Fe(IV) process with irreversibility due to second coordination sphere protonation change. The latter process is present in the Ga(III) complex and is assumed to be sulfonamide-based.

CONCLUSIONS

Our initial survey of the coordination chemistry of the new bis-sulfonamide ligand reveals that a wide variety of nuclearities, geometries, and protonation states are represented by the complexes reported here. Some of their features are worth emphasizing: All three deprotonated forms ($psmp^{3-}$, $psmpH^{2-}$, and $psmpH_2^-$) of the ligand have been observed, and notably, these can be prepared in the presence of water, even for the fully trideprotonated ligand when a divalent metal ion is employed. Apart from its anticipated ability to be involved in chelation, the deprotonated sulfonamide nitrogen atom can act as a bridging donor atom. Magnetic susceptibility measurements on $[Cu_3(psmp)_2(H_2O)]\cdot H_2O$ suggest that this rare bridging group is similar to a phenolato group in its ability to commute magnetic exchange coupling. Cyclic voltammetry suggests the +3 and +4 oxidation states may be accessible in the copper and the iron complexes, respectively.

The relatively low solubility of complexes and a propensity toward metal/ligand stoichiometry rearrangements has so far limited an exploration for the potential of these complexes for small molecule activation at their dimetallic sites. However, the series shows topological and structural properties relevant to these aims. The two dimetallic complexes, $[Cu_2(psmp)(OH)]$ and $[Cu_2(psmp)(OAc)_2]^-$ accommodate the two extremes in co-bridging ligands so far observed for a single μ_2-phenolato dimetal system: A single one-atom co-bridge (μ_2−OH) and two three-atom co-bridges (μ_2-OAc). Such a structural flexibility is interesting with respect to the potential of guest activation by dimetallic systems.[1] Furthermore the tricopper complex $[Cu_3(psmp)_2(H_2O)]$ shows an interesting topology. The auxiliary water ligand bound to the central copper ion is contained in a well-defined cleft whose four walls are constructed with two pyridine groups and two sulfonyl O atoms. Substitution of the water ligand with a sterically appropriate H-donor guest might lead to supramolecular activation chemistry since the guest can interact with the metal complex host via five contacts; one through copper ion coordination, two through π interactions with pyridyl rings, and two through H bonding or electrophilic interactions with sulfonyl O atoms. We will search for an appropriate guest. The structures of the 2:3 and 2:1 ligand/metal complexes $[Cu_3(psmp)_2(H_2O)]$ and $[M(psmpH)(psmpH_2)]$, where M = Ga(III), Fe(III), suggest the accessibility of bis-ligand mixed metal complexes using self-assembly and stepwise methods. The trinuclear complex $[Cu_3(psmp)_2(H_2O)]$ contains two chemically different metal coordination environments. This arrangement hints at the possible accessibility of structurally related heterotrimetallic complexes with the $[Cu_2M(psmp)_2(X)]$ formulation. For example, replacing the central Cu(II)−OH_2 (M−X) unit with a topologically similar V=O can be envisaged to give the analogously neutral and topologically similar $[Cu_2VO(psmp)_2]$. The preparation of this complex and other heterotrinuclear Cu_2/M and M′$_2$/M combinations may be of interest in the future development of the chemistry of this new class of ligand.

EXPERIMENTAL SECTION

Physical Measurements. ESI-MS spectra were recorded on a Bruker microTOF-QII. IR spectra were measured on a PerkinElmer Spectrum 65 equipped with a universal attenuated total reflection (ATR) sampling accessory. Solution ^1H and ^{13}C spectra were recorded on a Bruker 400 MHz using solvent residual peak as internal standard. Elemental analyses were performed at the Department of Chemistry, University of Copenhagen, Denmark. Melting point (m.p.) was determined on a Büchi 535. CVs were recorded in acetonitrile solution using an Autolab system (Eco Chemie, The Netherlands), controlled by GPES software. The working electrode was a Pt disk, the auxiliary electrode was a platinum wire, and the reference electrode was $Ag/AgNO_3$. As electrolyte, 0.1 M $TBAPF_6$ (TBA = tetrabutylammonium) was used. All measurements were calibrated versus the ferrocene/ferrocenium ($Fc^{0/+}$) redox couple $E_{1/2}$ = 0.44 V. CV spectra were recorded at a scan rate of 100 mV/s. The magnetic characterization was conducted on a Quantum Design MPMS-XL SQUID magnetometer equipped with a 5 T dc magnet. Dc susceptibility measurements were conducted on polycrystalline samples in polycarbonate capsules with a dc static field of 1000 Oe. The susceptibility was corrected for diamagnetic contributions from the compound by means of Pascal constants[16] and from the capsule (-5×10^{-7} cm^3 g^{-1}). The electron paramagnetic resonance (EPR) spectra were recorded on a Bruker Elexsys E500 equipped with a Bruker ER 4116 DM dual mode cavity, an EIP 538B frequency counter, an ESR9 cryostat, and a ER035 M NMR Gauss-meter.

General Information. Reagents and solvents were obtained commercially from Sigma Aldrich and used as received. The intermediate 2,6-dichlorosulfone-4-methylphenol was prepared using literature methods.[17]

Syntheses. *2,6-Bis(N-2-pyridylmethylsulfonamido)-4-methylphenol ($psmpH_3$).* A solution of 2-aminopyridine (1.4 mL, 1.5 g, 13 mmol) and triethylamine (1.8 mL, 1.3 g, 13 mmol) in dichloromethane (50 mL) was added slowly to a suspension of 2,6-dichlorosulfone-4-methylphenol (2.0 g, 6.5 mmol) in dichloromethane (50 mL). The resulting brown solution was stirred for approximately 16 h at RT, and the solvent was removed in vacuo. The residue was dissolved in a mixture of water (50 mL) and ethyl acetate (100 mL). The phases were separated, and the water phase was extracted with ethyl acetate (3 × 100 mL). The combined organic phases were dried over $MgSO_4$, and the solvent was removed in vacuo to yield 2,6-bis(*N*-2-pyridylmethylsulfonamido)-4-methylphenol (2.3 g, 5.2 mmol, 80%) as an off-white powder. m.p. 118.7−122.6°. Recrystallization from a mixture of EtOH and H_2O gave platelike X-ray quality crystals. ^1H NMR

dx.doi.org/10.1021/ic402599e | Inorg. Chem. 2014, 53, 2873−2882

Table 4. Selected Crystallographic Data

	psmpH$_3$	[Cu$_2$(psmp)(OH)]	[N(Et)$_3$CH$_2$Cl][Cu$_2$(psmp)-(OAc)$_2$]·2CH$_2$Cl$_2$	[Ga(psmpH)(psmpH$_2$)]·H$_2$O	[Fe(psmpH)(psmpH$_2$)]·3H$_2$O	[Cu$_3$(psmp)$_2$(H$_2$O)]·H$_2$O
empirical formula	$C_{19}H_{20}N_4O_5S_2$	$C_{38}H_{36}Cu_4N_8O_{12}S_4$	$C_{32}H_{44}Cl_5Cu_2N_5O_9S_2$	$C_{38}H_{38}GaN_8O_{11}S_4$	$C_{38}H_{38}FeN_8O_{13}S_4$	$C_{38}H_{38}Cu_3N_8O_{12}S_4$
formula weight (g/mol)	448.51	1179.15	1011.17	980.72	1002.37	1117.62
temperature (K)	150.0	150.0	150.0	150.0	150.0	293.0
crystal system	monoclinic	monoclinic	triclinic	monoclinic	monoclinic	monoclinic
space group	$P2_1/c$	$P2_1/n$	$P\bar{1}$	$P2_1/n$	$P2_1/n$	C_2/c
a, b, c (Å)	10.6396(7), 15.9476(10), 11.9430(8)	9.0921(6), 16.4521(10), 14.1333(9)	9.158(5), 19.566(5), 23.902(5)	10.1207(10), 21.195(2), 21.764(3)	10.0243(5), 21.3352(9), 21.2266(10)	25.662(4), 9.2714(14), 20.309(3)
α, β, γ (deg)	90, 101.216(4), 90	90, 108.384(3), 90	77.309(5), 82.883(5), 89.968(5)	90, 95.101(6), 90	90, 94.546(2), 90	90, 97.787(6), 90
volume (Å^3)	1987.7(2)	2006.2(2)	4144(3)	4650.2(9)	4525.5(4)	4787.4(13)
Z	4	2	4	4	4	4
ρ_{calc} (mg/mm^3)	1.499	1.952	1.621	1.401	1.471	1.551
abs. coefficient	0.309	2.378 mm^{-1}	1.506	0.835	0.589	1.560 mm^{-1}
F(000)	936.0	1192.0	2072.0	2020.0	2071.0	2272.0
crystal size (mm^3)	0.21 × 0.16 × 0.09	0.48 × 0.20 × 0.20	0.40 × 0.24 × 0.20	0.30 × 0.18 × 0.10	0.25 × 0.10 × 0.07	0.20 × 0.20 × 0.15
2θ range for data collection	3.902 to 52.742°	7.84 to 59.34°	5.98 to 55.12°	2.68 to 51.94°	3.818 to 52.802°	5 to 50°
index ranges	$-13 \le h \le 13$, $-19 \le k \le 19$, $-13 \le l \le 14$	$-12 \le h \le 12$, $-21 \le k \le 22$, $-19 \le l \le 19$	$-11 \le h \le 11$, $-25 \le k \le 25$, $-31 \le l \le 31$	$-12 \le h \le 12$, $0 \le k \le 26$, $0 \le l \le 26$	$-12 \le h \le 11$, $-25 \le k \le 26$, $-26 \le l \le 26$	$0 \le h \le 30$, $0 \le k \le 10$, $-24 \le l \le 23$
reflections collected	35 034	62 721	143 377	9060	41 238	4090
independent reflns (R_{int})	4055 (0.0545)	5596 (0.0256)	19 006 (0.0446)	9060	9288 (0.0480)	4090 (0.0000)
data/restraints/parameters	4055/3/331	5596/0/319	19 006/0/1003	9060/3/570	9288/5/612	4090/0/299
GOF on F^2	1.067	1.021	1.049	1.000	1.142	1.010
final $R_1(F)^a$ ($I > 2\sigma(I)$)/$wR_2(F^2)^b$	0.0357/0.0917	0.0224/0.0714	0.0621/0.1622	0.0720/0.1916	0.0398/0.1114	0.0445/0.1359
$R_1{}^a/wR_2(F^2)^b$ (all data)	0.0493/0.0994	0.0256/0.0741	0.0726/0.1702	0.1423/0.2135	0.0660/0.1391	0.0499/0.1395
largest diff. peak/hole/e Å^{-3}	0.33/−0.35	0.52/−0.30	1.43/−1.79	0.67/−0.94	0.78/−0.62	1.84/−0.48

$^a R_1(F) = \sum(||F_o| - |F_c||)/\sum|F_o|$. $^b wR_2(F^2) = \{\sum[w(F_o^2 - F_c^2)^2]/\sum[w(F_o^2)^2]\}^{1/2}$

dx.doi.org/10.1021/ic402599e | Inorg. Chem. 2014, 53, 2873−2882

(400 MHz, $CDCl_3$): δ (ppm) = 2.15 (s, 3H, CH_3), 4.07 (s, 4 H, CH_2), 7.02−7.04 (m, 2H, arom. H), 7.25 (d, 2H, J = 7.8 Hz, arom. H), 7.52−7.57 (m, 4H, arom. H), 8.31−8.33 (m, 2H, arom. H). ^{13}C NMR (100 MHz, $CDCl_3$): δ (ppm) = 19.9 (CH_3), 48.5 (CH_2), 120.5 (arom. C), 122.4 (arom. C), 122.6 (arom. C), 123.0 (arom. C), 127.5 (arom. C), 134.4 (arom. C), 136.7 (arom. C), 149.0 (arom. C), 156.1 (arom. C). ESI-MS pos. calcd (found) (m/z) = 449.10 (449.09, $[psmpH_3 + H]^+$, $C_{19}H_{21}N_4O_5S_2$, 100%). IR (Fourier transform (FT)-ATR diamond anvil) ν (cm^{-1}) = 1594 m, 1573 w, 1474 m, 1437 m, 1397 w, 1308 s, 1265 w, 1195 m, 1134 s, 1077 w, 1047 w, 997 w, 922 w, 887 w, 800 m, 753 s, 624 m, 565 s, 509 m, 478 w.

[Cu_2(psmp)(OH)]. Triethylamine (1 mL) was added under stirring to a suspension of $psmpH_3$ (100 mg, 0.22 mmol) in water (10 mL). The resulting solution was mixed with a solution of $Cu(NO_3)_2{\cdot}3H_2O$ (106 mg, 0.44 mmol) in water (10 mL) and allowed to stand overnight to form [Cu_2(psmp)(OH)] (58 mg, 0.1 mmol, 45%) as blue needles, which were washed with acetone and air-dried. Anal. Calcd for $C_{19}H_{18}Cu_2N_4O_6S_2$: C, 38.71; H, 3.08; N, 9.50. Found: C, 38.54; H, 3.04; N, 9.65%. IR (FT-ATR diamond anvil) ν (cm^{-1}) = 1608 m, 1485 w, 1433 s, 1354 w, 1283 w, 1264 m, 1252 m, 1234 m, 1220 m, 1140 m, 1100 s, 1081 s, 1050 m, 949 w, 876 w, 817 m, 777 m, 763 m, 743 m, 719 w, 683 m, 674 w, 660 m, 642 m, 603 w, 584 m, 559 w, 544 m, 523 m, 490 w, 465 m, 444 w, 418 m.

[$N(Et)_3CH_2Cl$][Cu_2(psmp)$(OAc)_2$]. $Cu(OAc)_2$ (175.6 mg, 0.88 mmol) was added to a solution of $psmpH_3$ (200 mg, 0.44 mmol) and triethylamine (3 mL) in dichloromethane (20 mL). The resulting suspension was refluxed overnight to form a dark greenish-brown solution. After cooling to RT the precipitate was collected by filtration, washed with ethanol, and air-dried to yield [$N(Et)_3CH_2Cl$]-[Cu_2(psmp)$(OAc)_2$] (177 mg, 0.21 mmol, 95%) as a bright-green powder. X-ray quality crystals of the dichloromethane solvate were formed by slow evaporation of the mother liquor. Anal. Calcd for $C_{30}H_{40}ClCu_2N_5O_9S_2$: C, 42.83; H, 4.79; N, 8.32. Found: C, 42.33; H, 4.61; N, 8.60%. ESI-MS neg. calcd (found) (m/z) = 690.95 (690.96, [Cu_2(psmp)$(OAc)_2$], $Cu_2C_{23}H_{23}N_4O_9S_2$, 100%), 630.93 (630.93, [Cu_2(psmp)(OAc)H], $Cu_2C_{21}H_{19}N_4O_7S_2$, 41%), 606.88 (606.89, [Cu_2(psmp) + HCl], $Cu_2C_{19}H_{16}N_4O_5S_2Cl$, 23%). IR (FT-ATR diamond anvil) ν (cm^{-1}) = 1614 m, 1601 m, 1479 w, 1439 m, 1410 s, 1336 w, 1279 w, 1244 m, 1148 m, 1115 w, 1096 s, 1049 w, 1049 w, 1028 w, 951 w, 880 w, 838 w, 814 w, 777 m, 765 m, 720 w, 678 m, 657 s, 596 m, 556 s, 537 w, 500 w, 453 w, 420 w.

[Cu_3(psmp)$_2$(H_2O)]·H_2O. A solution of NaOH (10%) in water (5 mL) was added to a solution of $CuSO_4{\cdot}5H_2O$ (83 mg, 0.33 mmol) in water (4 mL). The bright blue precipitate was collected by centrifugation, washed with cold water (5 × 6 mL), and suspended in MeOH (5 mL). This suspension was added to a solution of $psmpH_3$ (100 mg, 0.22 mmol) in MeOH (5 mL) and was allowed to stand without stirring for 3 d to form [$Cu_3(psmp)_2(H_2O)$] (65 mg, 0.06 mmol, 55%) as green crystals, which were separated from byproducts and remaining copper hydroxide by hand, washed with ethanol, and air-dried. Anal. Calcd for $C_{38}H_{38}Cu_3N_8O_{12}S_4$: C, 40.84; H, 3.43; N, 10.03. Found: C, 41.33; H, 3.69; N, 9.34%. ESI-MS pos. calcd (found) (m/z) = 1103.91 (1103.91, $[Cu_3(psmp)_2 + Na]^+$, $Cu_3C_{38}H_{34}N_8O_{10}S_4Na$, 36%), 1081.92 (1081.92, $[Cu_3(psmp)_2 + H]^+$, $Cu_3C_{38}H_{35}N_8O_{10}S_4$, 100%), 1042.99 (1042.99, $[Cu_2(psmpH)_2 + Na]^+$, $Cu_2C_{38}H_{36}N_8O_{10}S_4Na$, 88%), 1021.01 (1021.00, $[Cu_2(psmpH)_2 + H]^+$, $Cu_2C_{38}H_{37}N_8O_{10}S_4$, 85%), 610.92 (610.91, $[Cu_2(psmp)(OH) + Na]^+$, $Cu_2C_{19}H_{18}N_4O_6S_2Na$, 20%), 588.93 (588.93 $[Cu_2(psmp)(H_2O)]^+$, $Cu_2C_{19}H_{19}N_4O_6S_2$, 17%), 531.99 (531.99, $[Cu(psmpH) + Na]^+$, $CuC_{19}H_{18}N_4O_5S_2Na$, 54%), 510.01 (510.00, $[Cu(psmpH) + H]^+$, $CuC_{19}H_{19}N_4O_5S_2$, 38%). IR (FT-ATR diamond anvil) ν (cm^{-1}) = 1608 w, 1439 s, 1284 m, 1265 m, 1206 w, 1131 s, 1078 m, 1029 w, 939 w, 884 w, 811 m, 782 m, 757 s, 651 w, 631 w, 583 s, 529 m, 457 m.

[Ga(psmpH)(psmpH_2)]·H_2O. A solution of $Ga(NO_3)_3{\cdot}H_2O$ (100.0 mg, 0.39 mmol) in MeOH (5 mL) was added to a mixture of $pmspH_3$ (350.8 mg, 0.78 mmol, 2 equiv) and $NaOAc{\cdot}3H_2O$ (319.3 mg, 2.35 mmol) in MeOH/H_2O (20:5 v/v). The resulting clear yellow solution was allowed to stand in an open beaker at RT for 2 h, whereupon it started becoming cloudy. The beaker was sealed and left undisturbed overnight, after which an off-white crystalline mass had formed. The mixture was allowed to slowly cool to −40 °C, the mother liquor was decanted off, and the product was washed with ice-cold MeOH (3 × 5 mL) and air-dried (163.2 mg, 0.17 mmol, 42.7%). Anal. Calcd for $C_{38}H_{39}GaN_8O_{11}S_4$: C, 46.49; H, 4.00; N, 11.41. Found: C, 46.06; H, 3.42; N, 11.15%. ESI-MS pos. calcd (found) (m/z) = 963.08 (963.08, $[Ga(psmpH_2)_2]^+$, $C_{38}H_{38}GaN_8O_{10}S_4$, 100%), 985.07 (985.06, $[Ga(psmpH)(psmpH_2) + Na]^+$, $C_{38}H_{37}GaN_8NaO_{10}S_4$, 21%). IR (FT-ATR diamond anvil) ν (cm^{-1}) = 1602 w, 1573 w, 1442 m, 1322 m, 1275 m, 1205 w, 1125 s, 1052 m, 1025 w, 1008 w, 925 w, 860 m, 835 w, 805 m, 766 m, 652 m, 569 s, 533 m, 510 m.

[Fe(psmpH)(psmpH_2)]·2H_2O. $NH_4Fe(SO_4)_2{\cdot}12H_20$ (200.0 mg, 0.40 mmol) was dissolved in a mixture of MeOH (20 mL) and H_2O (10 mL). The bright yellow solution was combined with $psmpH_3$ (100.0 mg, 0.21 mmol) and triethylamine (0.1 mL) in MeOH (10 mL), whereupon it immediately turned dark red. Slow evaporation yielded needle-like red crystals, which were collected by filtration, washed with ice-cold MeOH (2 × 5 mL), and air-dried (62.7 mg, 0.06 mmol, 30.8%). Anal. Calcd for $C_{38}H_{41}FeN_8O_{12}S_4$: C, 46.30; H, 4.19; N, 11.37. Found: C, 46.86; H, 4.38; N, 11.20%. ESI-MS pos. calcd (found) (m/z) = 950.09 (950.09, $[Fe(psmpH_2)_2]^+$, $C_{38}H_{38}FeN_8O_{10}S_4$, 100%), 972.08 (972.08, $[Fe(psmpH)(psmpH_2) + Na]^+$, 48%), 1004.01 (1004.01 $[Fe_2(psmpH)_2]^+$, 76%). IR (FT-ATR diamond anvil) ν (cm^{-1}) = 1645 w, 1595 m, 1439 s, 130 m, 1210 m, 1150 m, 1105 s, 925 m, 815 m, 758 m, 665 w, 571 m.

Computational Modeling. For evaluation of the exchange couplings, the BS approach of Noodleman[18] as implemented in the ORCA version 2.8 suite of programs[19,20] was employed. The formalism of Yamaguchi,[21] which employs calculated expectation values $\langle S2 \rangle$ for both high-spin and BS states, was used. Calculations related to magnetic interactions have been performed using the PBE0 functional. The def2-TZVP basis function set from Alrichs was used.[22] Spin densities were visualized using the UCSF Chimera program version 1.5.3. The modeling of the magnetic data was performed with the MagProp program as included in the DAVE suite.[23]

Single-Crystal X-ray Diffraction. Selected crystallographic data are presented in Table 4. Diffraction data were collected using a Bruker-Nonius X8 APEX-II instrument (Mo Kα radiation, graphite monochromated fine-focused sealed tube), Oxford Agilent Supernova (Mo Kα radiation), or a Rigaku R-Axis IIC image-plate system (graphite monochromated Mo Kα radiation from a Rigaku RU-H3R rotating anode). Structure solutions were carried out with either SHELXS-97/2013[24] or SIR-92[25] and were refined against F^2 by full matrix least-squares using SHELXL-97/2013.[24] For $psmpH_3$, all hydrogen atoms were located in a difference Fourier map and refined with isotropic displacement parameters $U_{iso}(H) = 1.5U_{eq}$ when connected to hydroxyl or methyl groups and $U_{iso}(H) = 1.2U_{eq}$ for others. Sulfonamide H-atoms were constrained to a distance N···H of 0.91 ± 0.01 Å, and hydroxyl H atom was constrained to 0.84 ± 0.01 Å. For all other structures H atoms on C atoms were placed at calculated positions and allowed to ride during refinement. When possible, H atoms on sulfonamide/amine, coordinated hydroxo and/or water molecules were located in difference Fourier maps, and their positions were refined with restrained N/O−H distances or placed at calculated positions to form reasonable H bonds; subsequently, they were allowed to ride on the parent atom. Residual electron density, attributed to cocrystallized solvent molecules that was not possible to model satisfactorily in the structure of [Ga(psmpH)(psmpH$_2$)], was removed using the SQUEEZE-routine in PLATON.[26] Crystallographic data (excluding structure factors) for structures within this Paper have been deposited to the Cambridge Crystallographic Data Centre (CCDC 964331−964336).

■ ASSOCIATED CONTENT

Ⓢ Supporting Information

Complete crystallographic data (as CIF-files) for structures **1**−**6**; NMR, FT-IR, and ESI-MS spectra; discussion of magnetic properties of [$Cu_3(psmp)_2(H_2O)$]·H_2O. This material is available free of charge via the Internet at http://pubs.acs.org.

dx.doi.org/10.1021/ic402599e | Inorg. Chem. 2014, 53, 2873−2882

AUTHOR INFORMATION

Corresponding Author

*E-mail: mckenzie@sdu.dk. Phone: 45 6550 2518. Fax: (+45) 6615 8760.

Funding

The authors declare no competing financial interest in funding sources.

Notes

The authors declare no competing financial interest.

ACKNOWLEDGMENTS

This work was supported by the Danish Council for Independent Research | Natural Sciences. We thank Dr. Jason Price for assistance with part of the crystallographic studies.

REFERENCES

(1) (a) McKenzie, C. J.; Robson, R. *J. Chem. Soc., Chem. Commun.* **1988**, 122−114. (b) Liu, T.; Darensbourg, M. Y. *J. Chem. Soc.* **2007**, *129*, 7008−7009. (c) Gamba, I.; Palavicini, S.; Monzani, E.; Casella, L. *Chem.—Eur. J.* **2009**, *15*, 12932−12936. (d) Siewert, I.; Limberg, C.; Demeshko, S.; Hoppe, E. *Chem.—Eur. J.* **2008**, *14*, 9377−9388.

(2) (a) Grzybowski, J. J.; Merrell, P. H.; Urbach, F. L. *Inorg. Chem.* **1978**, *17*, 3078−3082. (b) Fallon, G. D.; Murray, K. S.; Spethmann, B.; Yandell, J. K.; Hodgkin, J. H.; Loft, B. C. *J. Chem. Soc., Chem. Commun.* **1984**, 1561−1563. (c) O'Connor, C. J.; Firmin, D.; Pant, A. K.; Babu, B. R.; Stevens, E. D. *Inorg. Chem.* **1986**, *25*, 2300−2307. (d) Mallah, T.; Boillot, M.-L.; Kahn, O.; Gouteron, J.; Jeannin, S.; Jeannin, Y. *Inorg. Chem.* **1986**, *25*, 3058−3065. (e) Higuchi, C.; Sakiyama, H.; Okawa, H.; Fenton, D. E. *J. Chem. Soc., Dalton Trans.* **1995**, 4015. (f) Borisovaa, N. E.; Reshetovaa, M. D.; Magdesievaa, T. V.; Khrustalevb, V. N.; Aleksandrovc, G. G.; Kuznetsova, M.; Skazovb, R. S.; Dolganova, Alexandr V.; Ikorskiyd, V. N.; Novotortsevc, V. M.; Eremenkoc, I. L.; Moiseevc, I. I.; Ustynyuka, Y. A. *Inorg. Chim Acta* **2008**, *361*, 2032−2044. (g) Gruenwald, K. R.; Volpe, M.; Moesch-Zanetti, N. C. *J. Coord. Chem.* **2012**, *65*, 2008−2020.

(3) Schindler, S.; Elias, H.; Paulus, H. *Z. Naturforsch., B: Chem. Sci.* **1990**, *45*, 607−618.

(4) Chanda, A.; Shan, X.; Mrinmoy Chakrabarti; Ellis, W. C.; Popescu, D. L.; Tiagode Oliveira, F.; Wang, D.; Que, L., Jr.; Collins, T. J.; Münck, E.; Bominaar, E. L. *Inorg. Chem.* **2008**, *47*, 3669−3678.

(5) Tiago de Oliveira, F.; Chanda, A.; Banerjee, D.; Shan, X.; Mondal, S.; Que, L.; Bominaar, E. L.; Münck, E.; Collins, T. J. *Science* **2007**, *315*, 835−838.

(6) (a) Chapman, R. L.; Stephens, F. S.; Vagg, R. S. *Inorg. Chim. Acta* **1980**, *43*, 29−33. (b) Barnes, D. J.; Stephens, F. S.; Vagg, R. S. *Inorg. Chim. Acta* **1980**, *51*, 155−162.

(7) Suksai, C.; Watchasit, S.; Tuntulani, T.; Pakawatchai, C. *Acta Crystallogr., Sect. E: Struct. Rep. Online* **2008**, *64*, 884−885.

(8) (a) Besenyei, G.; Párkányi, L.; Foch, I.; Simándi, L. I.; Kálmán, A. *Chem. Commun.* **1997**, 1143−1144. (b) Foch, I.; Párkányi, L.; Besenyei, G.; Simándi, L. I.; Kálmán, A. *J. Chem. Soc., Dalton Trans.* **1999**, 293−299. (c) Tejel, C.; Ciriano, M. A.; Jiménez, S.; Passarelli, V.; López, José A. *Inorg. Chem.* **2008**, *47*, 10220−10222.

(9) Otherwise known as nitrene or imido ligands, these are typically not prepared by in situ double deprotonation of a primary sulfonamide but are rather derived from azide or chloroamine precursors RSO_2N_3 and p-$MeC_6H_4SO_2NCl^-Na^+$, respectively.

(10) (a) González-Álvarez, M.; Pascual-Álvarez, A.; del Castillo Agudo, L.; Castiñeiras, A.; Liu-González, M.; Borrása, J.; Alzuet-Piña, G. *Dalton Trans.* **2013**, *42*, 10244−10259. (b) Tanakit, A.; Rouffet, M.; Martin, D. P.; Cohen, S. M. *Dalton Trans.* **2012**, *41*, 6507−6515. (c) Martin, D.; Rouffet, M.; Cohen, S. M. *Inorg. Chem.* **2010**, *49*, 10226−10228.

(11) (a) Veltzé, S.; Kirk Egdal, R.; Johansson, F. B.; Bond, A. D.; McKenzie, C. J. *Dalton Trans.* **2009**, 10495−10504. (b) Egdal, R. K.; Johansson, F. B.; Veltzé, S.; Skou, E.; Bond, A. D.; McKenzie, C. J. *Dalton Trans.* **2011**, *40*, 3336−3345.

(12) Nakamoto, K. *Infrared and Raman Spectra of Inorganic and Coordination Compounds, Part B;* Wiley Interscience: Hoboken, NJ, 1997; p 60.

(13) (a) Wrigth, D.; Wulff, C. *J. Org. Chem.* **1970**, *35*, 4252−4252. (b) Almarzoqi, B.; George, A. V.; Isaacs, N. S. *Tetrahedron* **1986**, *42*, 601−601. (c) Mas, M.; Sola, J.; Solans, X.; Aguilo, M. *Inorg. Chim. Acta.* **1987**, *133*, 217−219.

(14) (a) Menabue, L.; Saladini, M. *Inorg. Chem.* **1991**, *30*, 1651−1655. (b) Goodwin, J. M.; Chiang, P.-C.; Brynda, M.; Penkina, K.; Olmstead, M. M.; Patten, T. E. *Dalton Trans.* **2007**, 3086−3092. (c) Ishiwata, K.; Kuwata, S.; Ikiraya, T. *J. Am. Chem. Soc.* **2009**, *131*, 5001−5009.

(15) Sanmartín, J.; Novio, F.; García-Deibe, A. M.; Fondo, M.; Ocampo, N.; Bermejo, M. R. *Eur. J. Inorg. Chem.* **2008**, 1719−1726.

(16) (a) Bain, G. A.; Berry, J. F. *J. Chem. Educ.* **2008**, *85*, 532−536. (b) Gutierrez, L.; Alzuet, G.; Real, J. A.; Cano, J.; Borras, J.; Castineiras, A. *Inorg. Chem.* **2000**, *39*, 3608−3614. (c) Gutierrez, L.; Alzuet, G.; Borras, J.; Liu-Gonzalez, M.; Sanz, F.; Castineiras, A. *Polyhedron* **2001**, *20*, 703−709. (d) Congreve, A.; Kataky, R.; Knell, M.; Parker, D.; Puschmann, H.; Senanayake, K.; Wylie, L. *New J. Chem.* **2003**, *27*, 98−106. (e) Duran, M. L.; Garcia-Vazquez, J. A.; Gomez, C.; Sousa-Pedrares, A.; Romero, J.; Sousa, A. *Eur. J. Inorg. Chem.* **2002**, 2348−2354.

(17) Pollak, J.; Gebauer-Füllneg, E.; Riesz, E. *Monatsh. Chem.* **1925**, *46*, 383−397.

(18) Noodleman, L. *J. Chem. Phys.* **1981**, *74*, 5737−5743.

(19) Neese, F. *ORCA,* Version 2.8, Revision 2131; Institut für Physikalische und Theoretische Chemie, Universität Bonn: Germany, 2010.

(20) (a) Neese, F. *Coord. Chem. Rev.* **2009**, *253*, 526−563. (b) Sinnecker, F.; Neese, F.; W. Lubitz, W. *J. Biol. Inorg. Chem.* **2005**, *10*, 231−238.

(21) (a) Yamaguchi, K.; Takahara, Y.; Fueno, T. In *Applied Quantum Chemistry;* Smith, V. H.; Schafer, F.; III, Morokuma, K., Eds.; D. Reidel: Boston, MA, 1986; p 155. (b) Soda, T.; Kitagawa, Y.; Onishi, T.; Takano, Y.; Shigeta, Y.; Nagao, H.; Yoshioka, Y.; Yamaguchi, K. *Chem. Phys. Lett.* **2000**, *319*, 223−230.

(22) Weigend, F.; Ahlrichs, R. *Phys. Chem. Chem. Phys.* **2005**, *7*, 3297−3305.

(23) Azuah, R.; Copley, J.; Dimeo, R.; Park, S.; Lee, S.-H.; Munter, A.; Kneller, L.; Qiu, Y.; Peral, I.; Brown, C.; Kienzle, P.; Tregenna-Piggott, P. L. W. *Dave* 1.4 Beta. (http://www.ncnr.nist.gov/dave) (Accessed June 1, 2011).

(24) Sheldrick, G. M. *Acta Crystallogr.* **2008**, *A64*, 112−122.

(25) Altomare, A.; Cascarano, G.; Giacovazzo, C.; Guagliardi, A.; Burla, M. C.; Polidori, G.; Camalli, M. J. *J. Appl. Crystallogr.* **1994**, *27*, 435−436.

(26) Spek, A. L. *Acta Crystallogr.* **2009**, *D65*, 148−155.